J. Fluid Mech. (2004), *vol.* 509, *pp.* 125–144.
DOI: 10.1017/S0022112004009024 Printed in the United Kingdom

Instability due to a discontinuity in magnetic diffusivity in the presence of magnetic shear

By S. N. BHATTACHARYYA[1] AND A. S. GUPTA[2]

[1]Department of Mechanical Engineering, Indian Institute of Technology, Kharagpur 721 302, West Bengal, India

[2]Department of Mathematics, Indian Institute of Technology, Kharagpur 721 302, West Bengal, India

(Received 14 March 2003 and in revised form 10 February 2004)

The linear stability of two viscous electrically conducting quiescent fluids, separated by a plane interface, and permeated by a sheared magnetic field parallel to the interface is studied. An analytical study using a short-wavelength approximation shows that, in the absence of surface tension, if the magnetic field vanishes on the unperturbed interface, the configuration is always unstable provided the magnetic diffusivities of the two fluids are different. When the unperturbed magnetic field does not vanish on the interface it may stabilize or destabilize the configuration depending on the values of certain parameters. The growth rates for the instability obtained using a short-wavelength approximation are shown to be in good agreement with the results obtained by numerical solution. The numerical study further shows that the instability has maximum growth rate for wavenumbers of order unity and persists even for long-wavelength perturbations. A physical explanation for the instability is provided.

1. Introduction

It was first shown by Yih (1967) that an instability can occur when two co-flowing fluids have different viscosities. He considered plane Couette–Poiseuille flow of two superposed layers of fluid and showed that a long-wavelength instability occurs, which persists for arbitrarily small values of the Reynolds number, provided the two fluids have different viscosities. This work was further extended to three fluid layers (Li 1969) and to cylindrical geometry (Hickox 1971). However, it was not clear whether the instability was attributable to the presence of rigid boundaries, as in the classical problem of stability of plane Poiseuille flow of a homogeneous fluid (Lin 1955; Drazin & Reid 1981), or to the jump in viscosity across the interface. This prompted Hooper & Boyd (1983) to carry out a stability analysis of an unbounded flow configuration in which two viscous fluids occupying the half spaces $y' > 0$ and $y' < 0$, have a velocity field given by $(a_1 y', 0, 0)$ for $y' > 0$ and $(a_2 y', 0, 0)$ for $y' < 0$, a_1 and a_2 being two constants of the two shearing flows, which satisfy $\mu_1 a_1 = \mu_2 a_2$, where μ_1 and μ_2 are the viscosities of the two fluids. They showed that when the two fluids have equal densities and the surface tension at the interface is neglected, the configuration is unstable to short wavelength perturbations provided the viscosities of the two fluids are different. A physical explanation for this instability was provided by Hinch (1984). More recently, this instability was also confirmed by numerical simulations (Li, Renardy & Renardy 1998; Renardy & Li 1999).

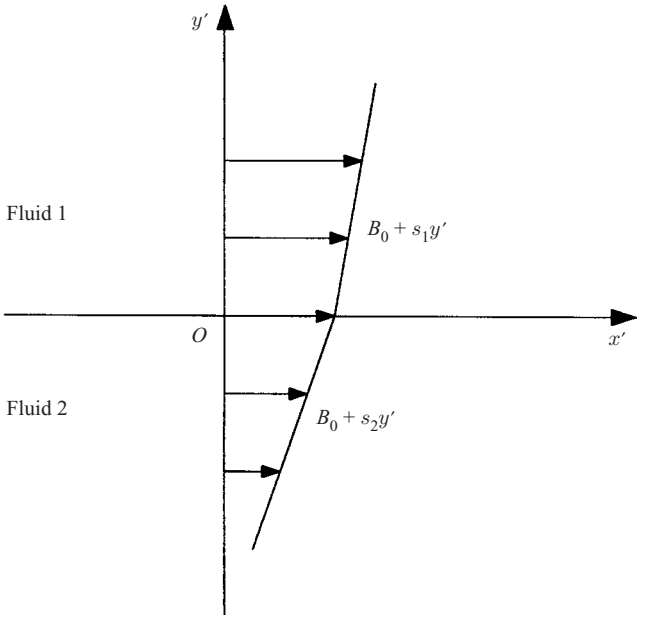

FIGURE 1. A sketch of the physical problem.

In this paper, we discuss a similar but new kind of instability. We consider an unbounded configuration of two viscous electrically conducting fluids, both of which are at rest initially and are permeated by a sheared magnetic field parallel to the interface, and study the stability of this configuration to two-dimensional perturbations. The two fluids, identified by subscripts 1 and 2, occupy the half spaces $y' > 0$ and $y' < 0$ as shown in figure 1. The magnetic shears s_1 and s_2 are constants and B_0 is the magnetic field at the interface. We assume that the shears s_1 and s_2 are positive and B_0 is non-negative. This can be ensured by a suitable choice of the coordinate system. Further, λ_1 and λ_2 are the magnetic diffusivities of the two fluids. Following Hooper & Boyd (1983), we first carry out a perturbative study for short-wavelength disturbances. We find that a discontinuity in magnetic diffusivity in the presence of a magnetic shear can give rise to an instability. A condition for the stability of the configuration is derived. If we assume that the fluids are non-magnetic, the magnetic diffusivities of the two fluids will be different provided their electrical conductivities are different and we can, therefore, say that the instability is due to a discontinuity in the electrical conductivity. In order to confirm the predictions of the short wavelength analysis, we carry out a numerical study which does not make an assumption of short wavelength. This shows that the instability is not restricted to short wavelengths.

A magnetic field has been shown to have a stabilizing effect on many hydrodynamic instabilities. It was shown that the Kelvin–Helmholtz instability can be stabilized by a constant magnetic field parallel to the direction of flow (Chandrasekhar 1981) or by a crossed magnetic field parallel to the interface (Fejer 1964). In the present study, we find, by contrast, that in the presence of a discontinuity in the electrical conductivity, under certain conditions, a sheared magnetic field can give rise to a new instability.

Stratification of electrical conductivity is known to cause instability in the presence of electric current. For two superposed fluids of different electrical conductivities Sneyd (1985, 1992), Sneyd & Wang (1994) and Davidson & Lindsay (1998) had

studied the stability of the configuration in the context of aluminium reduction cells and shown that under certain conditions an instability can occur when there is an equilibrium current in a direction normal to the interface between the two fluids. Again a continuous variation in electrical conductivity in the presence of a sheared magnetic field is known to give rise to a rippling instability (Furth, Killeen & Rosenbluth 1963; White 1989). However, the instability analysed in this paper is different from these earlier studies. This is discussed in more detail in § 6.

In § 2, we give a mathematical formulation of the stability problem; in § 3, we carry out a regular perturbation analysis of the stability problem for disturbances of short wavelength; and in § 4, we carry out a numerical solution using the finite-difference method, the details of the numerical method are given in the Appendix. In § 5, we give a physical explanation of the mechanism of instability along with a description of the experimental set-up for the realization of a sheared magnetic field in the two fluids. A discussion of the results is given in § 6.

2. Formulation of the stability problem

We consider a configuration of two quiescent, viscous, electrically conducting fluids in the presence of a sheared magnetic field shown in figure 1. We assume both fluids are incompressible. The governing equations in each fluid are (Shercliff 1965)

$$\frac{\partial \boldsymbol{v}}{\partial t'} + \boldsymbol{v}\cdot\nabla\boldsymbol{v} = -\frac{1}{\rho}\nabla p^* + \frac{1}{\rho\mu_0}\boldsymbol{B}\cdot\nabla\boldsymbol{B} + \nu\nabla^2\boldsymbol{v}, \tag{2.1}$$

$$\frac{\partial \boldsymbol{B}}{\partial t'} + \boldsymbol{v}\cdot\nabla\boldsymbol{B} = \boldsymbol{B}\cdot\nabla\boldsymbol{v} + \lambda\nabla^2\boldsymbol{B}, \tag{2.2}$$

$$\nabla\cdot\boldsymbol{v} = 0, \tag{2.3}$$

$$\nabla\cdot\boldsymbol{B} = 0, \tag{2.4}$$

where ρ, ν and λ are the density, kinematic viscosity and magnetic diffusivity of the fluid, $\boldsymbol{v}$ is the fluid velocity, $\boldsymbol{B}$ is the magnetic field, p^* is the total (fluid + magnetic) pressure and μ_0 is the permeability of a vacuum. We consider an unperturbed state given by

$$\boldsymbol{v} = \boldsymbol{0}, \quad \boldsymbol{B} = (B_0 + sy', 0), \quad p^* = p_0, \tag{2.5}$$

where B_0, s and p_0 are constants. It can be readily shown that (2.5) is consistent with (2.1)–(2.4). We now consider a two-dimensional perturbation from (2.5) given by

$$\boldsymbol{v} = (u',\ v'), \quad \boldsymbol{B} = (B_0 + sy' + b'_x,\ b'_y), \quad p^* = p_0 + p', \tag{2.6}$$

where u', v', b'_x, b'_y and p' are functions of x', y' and t'. The reason for restricting our study to two-dimensional perturbations and its limitations are discussed in § 6. Substituting from (2.6) into (2.1)–(2.4), linearizing in the perturbations, and assuming normal modes with (x', t')-dependence of the form $\exp[\mathrm{i}\alpha'(x' - c't')]$, we obtain

$$-\mathrm{i}\alpha' c' u' = -\frac{1}{\rho}\,\mathrm{i}\alpha' p' + \frac{1}{\rho\mu_0}(B_0 + sy')\mathrm{i}\alpha' b'_x + \frac{sb'_y}{\rho\mu_0} + \nu\left(\frac{\mathrm{d}^2}{\mathrm{d}y'^2} - \alpha'^2\right)u', \tag{2.7}$$

$$-\mathrm{i}\alpha' c' v' = -\frac{1}{\rho}\,\frac{\mathrm{d}p'}{\mathrm{d}y'} + \frac{1}{\rho\mu_0}(B_0 + sy')\mathrm{i}\alpha' b'_y + \nu\left(\frac{\mathrm{d}^2}{\mathrm{d}y'^2} - \alpha'^2\right)v', \tag{2.8}$$

$$-\mathrm{i}\alpha' c' b'_x + sv' = (B_0 + sy')\mathrm{i}\alpha' u' + \lambda\left(\frac{\mathrm{d}^2}{\mathrm{d}y'^2} - \alpha'^2\right)b'_x, \tag{2.9}$$

$$-\mathrm{i}\alpha' c' b'_y = (B_0 + sy')\mathrm{i}\alpha' v' + \lambda\left(\frac{\mathrm{d}^2}{\mathrm{d}y'^2} - \alpha'^2\right) b'_y, \tag{2.10}$$

$$\mathrm{i}\alpha' u' + \frac{\mathrm{d}v'}{\mathrm{d}y'} = 0, \tag{2.11}$$

$$\mathrm{i}\alpha' b'_x + \frac{\mathrm{d}b'_y}{\mathrm{d}y'} = 0. \tag{2.12}$$

We now consider the boundary conditions at the interface between the two fluids. In the unperturbed state, balance of normal stress and continuity of the tangential component of the magnetic field require p_0 and B_0 to have the same value in the two fluids, while continuity of the tangential component of electric field requires

$$\lambda_1 s_1 = \lambda_2 s_2. \tag{2.13}$$

Let $y' = \eta'(x', t')$ be the equation of the interface between the two fluids in the perturbed state. The kinematic boundary condition at the interface, after linearizing and assuming normal modes as before, gives

$$v' = -\mathrm{i}\alpha' c' \eta' \quad \text{at} \quad y' = 0. \tag{2.14}$$

We now impose the requirement of continuity of the tangential and normal components of velocity, shear and normal stress, tangential and normal components of the magnetic field and tangential component of the electric field at the perturbed interface. Again linearizing and assuming normal modes we have

$$u'_1 = u'_2 \quad \text{at} \quad y' = 0, \tag{2.15}$$

$$v'_1 = v'_2 \quad \text{at} \quad y' = 0, \tag{2.16}$$

$$\mu_1\left(\frac{\mathrm{d}u'_1}{\mathrm{d}y'} + \mathrm{i}\alpha' v'_1\right) = \mu_2\left(\frac{\mathrm{d}u'_2}{\mathrm{d}y'} + \mathrm{i}\alpha' v'_2\right) \quad \text{at} \quad y' = 0, \tag{2.17}$$

$$-p'_1 + 2\mu_1\frac{\mathrm{d}v'_1}{\mathrm{d}y'} - T\alpha'^2\eta' = -p'_2 + 2\mu_2\frac{\mathrm{d}v'_2}{\mathrm{d}y'} \quad \text{at} \quad y' = 0, \tag{2.18}$$

$$s_1\eta' + b'_{1x} = s_2\eta' + b'_{2x} \quad \text{at} \quad y' = 0, \tag{2.19}$$

$$b'_{1y} = b'_{2y} \quad \text{at} \quad y' = 0, \tag{2.20}$$

$$\lambda_1\left(\mathrm{i}\alpha' b'_{1y} - \frac{\mathrm{d}b'_{1x}}{\mathrm{d}y'}\right) = \lambda_2\left(\mathrm{i}\alpha' b'_{2y} - \frac{\mathrm{d}b'_{2x}}{\mathrm{d}y'}\right) \quad \text{at} \quad y' = 0. \tag{2.21}$$

In (2.18), T is the surface tension, assumed constant. Equation (2.19) is written on the assumption that the permeabilities of the two fluids are equal, which is true if both fluids are assumed to be non-magnetic. In deriving (2.21), the boundary condition (2.13) has been used. Finally, the perturbations must vanish as $y' \to \pm\infty$.

We now introduce a streamfunction $\psi(y')$ and a similar function $\phi(y')$ for the magnetic field such that

$$u' = \frac{\mathrm{d}\psi}{\mathrm{d}y'}, \quad v' = -\mathrm{i}\alpha'\psi, \tag{2.22}$$

$$b'_x = \frac{\mathrm{d}\phi}{\mathrm{d}y'}, \quad b'_y = -\mathrm{i}\alpha'\phi. \tag{2.23}$$

Equations (2.11) and (2.12) are now identically satisfied. We now write the linearized equations in terms of ψ and ϕ. Eliminating p' from (2.7) and (2.8) and using (2.22) and (2.23), we obtain

$$-\mathrm{i}\alpha' c'\left(\frac{\mathrm{d}^2}{\mathrm{d}y'^2}-\alpha'^2\right)\psi = \frac{\mathrm{i}\alpha'}{\rho\mu_0}(B_0+sy')\left(\frac{\mathrm{d}^2}{\mathrm{d}y'^2}-\alpha'^2\right)\phi+\nu\left(\frac{\mathrm{d}^2}{\mathrm{d}y'^2}-\alpha'^2\right)^2\psi. \quad (2.24)$$

Substituting (2.22) and (2.23) into (2.10), we obtain

$$-\mathrm{i}\alpha' c'\phi = \mathrm{i}\alpha'(B_0+sy')\psi+\lambda\left(\frac{\mathrm{d}^2}{\mathrm{d}y'^2}-\alpha'^2\right)\phi. \quad (2.25)$$

The equation we obtain by substituting (2.22) and (2.23) into (2.9) is identical to the equation obtained by differentiating (2.25) with respect to y' and is, therefore, redundant. Of the boundary conditions (2.15) – (2.21), it can be shown that (2.21) is redundant. To see this we substitute (2.23) into (2.21) to obtain

$$\lambda_1\left(\frac{\mathrm{d}^2}{\mathrm{d}y'^2}-\alpha'^2\right)\phi_1=\lambda_2\left(\frac{\mathrm{d}^2}{\mathrm{d}y'^2}-\alpha'^2\right)\phi_2 \quad \text{at} \quad y'=0. \quad (2.26)$$

Using (2.25), it is seen that this condition follows from $\psi_1=\psi_2$ and $\phi_1=\phi_2$ at $y'=0$ which are required by (2.16) and (2.20). The remaining boundary conditions (2.15)–(2.20) can be expressed in terms of ψ and ϕ by substituting for p' from (2.7), η' from (2.14) and using (2.22) and (2.23). Therefore, equations (2.24) and (2.25) in the two fluids, the boundary conditions (2.15)–(2.20), written in terms of ψ and ϕ, and the requirement that the perturbations vanish as $y'\to\pm\infty$, together constitute the eigenvalue problem governing linear stability.

The geometry of the problem does not define a length scale. Following Hooper & Boyd (1983) we define a length scale $(\lambda_2(\mu_0\rho_2)^{1/2}/s_2)^{1/2}$ and a time scale $(\mu_0\rho_2)^{1/2}/s_2$ and introduce non-dimensional variables

$$(X,Y,1/\alpha)=\left(\frac{s_2^2}{\lambda_2^2\mu_0\rho_2}\right)^{1/4}(x',y',1/\alpha'), \quad C=\left(\frac{\mu_0\rho_2}{s_2^2\lambda_2^2}\right)^{1/4}c'. \quad (2.27)$$

Further, we define

$$(f_1,f_2)=\left(\frac{1}{\mu_0\rho_2}\right)^{1/2}(\phi_1,\phi_2), \quad (2.28)$$

so that f_1 and f_2 have the same dimension as ψ_1 and ψ_2. Typically, for interfacial modes, the length scale normal to the interface is proportional to the wavelength. Therefore, following Hooper & Boyd (1983), for convenience, we define rescaled coordinates and a rescaled phase speed by

$$(x,y)=\alpha(X,Y), \quad C_1=\alpha C. \quad (2.29)$$

Substituting from (2.27)–(2.29) into (2.24) and (2.25) and writing the equations separately for the two fluids, we have

$$\left(\frac{\mathrm{d}^2}{\mathrm{d}y^2}-1\right)^2\psi_1=-\mathrm{i}\alpha^{-2}\frac{m}{rP_2}\left[C_1\left(\frac{\mathrm{d}^2}{\mathrm{d}y^2}-1\right)\psi_1+r(\alpha M+\chi y)\left(\frac{\mathrm{d}^2}{\mathrm{d}y^2}-1\right)f_1\right], \quad (2.30)$$

$$\left(\frac{\mathrm{d}^2}{\mathrm{d}y^2}-1\right)^2\psi_2=-\mathrm{i}\alpha^{-2}\frac{1}{P_2}\left[C_1\left(\frac{\mathrm{d}^2}{\mathrm{d}y^2}-1\right)\psi_2+(\alpha M+y)\left(\frac{\mathrm{d}^2}{\mathrm{d}y^2}-1\right)f_2\right], \quad (2.31)$$

$$\left(\frac{\mathrm{d}^2}{\mathrm{d}y^2}-1\right) f_1 = -\mathrm{i}\alpha^{-2}\chi\,[C_1 f_1 + (\alpha M + \chi y)\psi_1], \tag{2.32}$$

$$\left(\frac{\mathrm{d}^2}{\mathrm{d}y^2}-1\right) f_2 = -\mathrm{i}\alpha^{-2}[C_1 f_2 + (\alpha M + y)\psi_2]. \tag{2.33}$$

Similarly, writing boundary conditions (2.15)–(2.20) in terms of ψ and ϕ and using (2.27)–(2.29), we obtain

$$\psi_1 - \psi_2 = 0 \quad \text{at} \quad y = 0, \tag{2.34}$$

$$\frac{\mathrm{d}\psi_1}{\mathrm{d}y} - \frac{\mathrm{d}\psi_2}{\mathrm{d}y} = 0 \quad \text{at} \quad y = 0, \tag{2.35}$$

$$\left(\frac{\mathrm{d}^2}{\mathrm{d}y^2}+1\right)\psi_1 - m\left(\frac{\mathrm{d}^2}{\mathrm{d}y^2}+1\right)\psi_2 = 0 \quad \text{at} \quad y = 0, \tag{2.36}$$

$$\begin{aligned}
&\frac{P_2}{m}\left(\frac{\mathrm{d}^2}{\mathrm{d}y^2}-3\right)\frac{\mathrm{d}\psi_1}{\mathrm{d}y} - P_2\left(\frac{\mathrm{d}^2}{\mathrm{d}y^2}-3\right)\frac{\mathrm{d}\psi_2}{\mathrm{d}y} \\
&\quad = -\mathrm{i}\alpha^{-2}\left[\frac{C_1}{r}\frac{\mathrm{d}\psi_1}{\mathrm{d}y} + \alpha M\frac{\mathrm{d}f_1}{\mathrm{d}y} - \chi f_1 - \frac{S\alpha^3}{(\chi-1)}\frac{\mathrm{d}f_1}{\mathrm{d}y}\right] \\
&\quad\quad + \mathrm{i}\alpha^{-2}\left[C_1\frac{\mathrm{d}\psi_2}{\mathrm{d}y} + \alpha M\frac{\mathrm{d}f_2}{\mathrm{d}y} - f_2 - \frac{S\alpha^3}{(\chi-1)}\frac{\mathrm{d}f_2}{\mathrm{d}y}\right] \quad \text{at} \quad y = 0,
\end{aligned} \tag{2.37}$$

$$C_1\left(\frac{\mathrm{d}f_2}{\mathrm{d}y} - \frac{\mathrm{d}f_1}{\mathrm{d}y}\right) - (\chi-1)\psi_1 = 0 \quad \text{at} \quad y = 0, \tag{2.38}$$

$$f_1 - f_2 = 0 \quad \text{at} \quad y = 0. \tag{2.39}$$

Here,

$$\begin{aligned}
&m = \frac{\mu_2}{\mu_1}, \quad r = \frac{\rho_2}{\rho_1}, \quad \chi = \frac{\lambda_2}{\lambda_1} = \frac{s_1}{s_2}, \quad P_2 = \frac{\nu_2}{\lambda_2}, \\
&M = \frac{B_0}{\left(\mu_0\rho_2\lambda_2^2 s_2^2\right)^{1/4}}, \quad S = \frac{T}{\lambda_2\rho_2}\left(\frac{\mu_0\rho_2}{s_2^2\lambda_2^2}\right)^{1/4},
\end{aligned} \tag{2.40}$$

where M and S are the magnetic and surface tension parameters. In deriving (2.37), we have used (2.38). Further,

$$\psi_1 \to 0, \ f_1 \to 0 \quad \text{as} \quad y \to \infty; \qquad \psi_2 \to 0, \ f_2 \to 0 \quad \text{as} \quad y \to -\infty. \tag{2.41}$$

It may be noticed that there is another length scale in the problem, given by B_0/s_2 and the parameter M is the ratio of this length scale to the length scale $(\lambda_2^2\mu_0\rho_2/s_2^2)^{1/4}$ which we have used for defining non-dimensional variables.

3. A regular perturbation analysis for short wavelength

It is clear from the form of equations (2.30)–(2.33) and the boundary conditions (2.34)–(2.39) that $1/\alpha^2$ can be used as an expansion parameter for carrying out a regular perturbation analysis for disturbances of short wavelength. Accordingly, we

assume the expansions

$$\left.\begin{aligned} \psi_1(y) &= \sum_{n=0}^{\infty} \frac{a_n(y)}{\alpha^{2n}}\,\mathrm{e}^{-y}, \quad \psi_2(y) = \sum_{n=0}^{\infty} \frac{b_n(y)}{\alpha^{2n}}\,\mathrm{e}^{y}, \\ f_1(y) &= \sum_{n=0}^{\infty} \frac{g_n(y)}{\alpha^{2n}}\,\mathrm{e}^{-y}, \quad f_2(y) = \sum_{n=0}^{\infty} \frac{d_n(y)}{\alpha^{2n}}\,\mathrm{e}^{y}, \\ C_1 &= \sum_{n=0}^{\infty} \frac{c_n}{\alpha^{2n}}. \end{aligned}\right\} \tag{3.1}$$

As in Hooper & Boyd (1983), the factors e^{-y} and e^{y}, though not essential, are retained for convenience. We further assume that $\alpha M = O(1)$ and $\alpha^3 S = O(1)$. Using (2.27) and (2.40), the first assumption can be written as $\alpha' B_0/s_2 = O(1)$, in other words, the wavelength of the perturbation is of the same order as the length scale B_0/s_2. We substitute from (3.1) into (2.30)–(2.39) and (2.41) and carry out the analysis order by order exactly as in Hooper & Boyd (1983). To zeroth order, we obtain

$$a_0(y) = 0, \quad b_0(y) = 0, \quad g_0 = K_0, \quad d_0 = K_0, \quad c_0 = 0, \tag{3.2}$$

where K_0 is a non-zero constant. Proceeding to the next order, we obtain

$$c_1 = \frac{\mathrm{i}}{4P_2}\left(\frac{m}{1+m}\right)[2\alpha M(\chi-1) + (\chi-1)^2 - 2S\alpha^3]. \tag{3.3}$$

We may proceed to higher-order approximations in α^{-2}, but (3.3) seems adequate for discussing the instability of the mode. It can readily be seen that to $O(\alpha^{-2})$ the configuration will be stable or unstable depending on whether

$$2\alpha M(\chi-1) + (\chi-1)^2 - 2S\alpha^3 < \quad \text{or} \quad > 0. \tag{3.4}$$

This shows that if surface tension is absent ($S = 0$) and the magnetic field vanishes at the unperturbed interface ($M = 0$), the configuration is always unstable provided the two fluids have different magnetic diffusivities ($\chi \neq 1$). When the magnetic field does not vanish on the unperturbed interface ($M \neq 0$), it may have a stabilizing or destabilizing effect depending on the sign of M, i.e. on the direction of the magnetic field at the unperturbed interface. Surface tension always has a stabilizing effect. A shear in the magnetic field is necessary for this instability to occur. This is not obvious from (3.3) because it has been obtained after scaling which involves the magnetic shear. From (2.27), (2.29) and (3.1)–(3.3), we find that the dimensional growth rate, correct to first order in $1/\alpha^2$, is

$$\alpha' c' = \left(\frac{s_2^2}{\mu_0 \rho_2}\right)^{1/2} \frac{1}{\alpha^3} \frac{\mathrm{i}}{4P_2}\left(\frac{m}{1+m}\right)[2\alpha M(\chi-1) + (\chi-1)^2 - 2S\alpha^3]. \tag{3.5}$$

From this expression, it can readily be seen that the growth rate vanishes when $s_2 = 0$. Further, it should be kept in mind that the condition for stability or instability, given by (3.4), holds, provided the magnetic shears s_1 and s_2 are positive. This does not cause loss of generality because the coordinate system can be suitably chosen to make the magnetic shears positive. It may be further observed that a jump in viscosity at the interface is not essential for this instability to occur and, as seen from (3.3), instability can occur even for $m = 1$. We also notice that when $\chi = 1$ (i.e. no jump in the magnetic diffusivities at the interface) there can be no instability of the interface. Therefore, a difference in the magnetic diffusivities of the two fluids is essential for the

	Im(C_1)	
α	Numerical	Short wavelength
10	0.04850	0.05
20	0.01247	0.0125
30	0.005549	0.005556
40	0.003122	0.003125

TABLE 1. Effect of wavenumber α on the growth rate Im(C_1) for $r=1$, $m=1$, $\chi=2$, $S=0$, $M=0$ and $P_2=0.025$.

instability studied in this manuscript to occur. It may be mentioned that in this study, since our focus is on the effect of a jump in magnetic diffusivities at the interface on the stability of the configuration, we have not considered the effect of gravity. If this were taken into account, we would expect a stabilizing or destabilizing effect depending on whether the lighter or heavier fluid is on top. Equation (3.3) for the growth rate would be valid in its present form either in zero gravity or in the presence of gravity if the two fluids have equal densities.

4. A numerical solution for linear stability

In this section, we shall solve the equations governing linear stability without making a short-wavelength approximation. Hooper & Boyd (1983) had used an exact solution of the linearized equation in each fluid in terms of an Airy function. However, in our study where, in each fluid, we have two coupled equations for ψ and f, we have not been able to find an exact closed-form solution. Instead, we use the finite-difference method to convert the governing system, comprising of equations (2.30)–(2.33), together with boundary conditions (2.34)–(2.39) and (2.41), to a generalized matrix eigenvalue problem $\boldsymbol{A}\boldsymbol{x}=C_1\boldsymbol{B}\boldsymbol{x}$, where $\boldsymbol{A}$ and $\boldsymbol{B}$ are complex square matrices, C_1, the growth rate, is the eigenvalue and $\boldsymbol{x}$, the eigenvector, contains values of ψ and f at different grid-points. Since the equations are to be solved on an infinite domain with the requirement that the solutions vanish asymptotically at infinity, for the finite-difference scheme we choose a large value y_{max} and assume that for $|y|>y_{max}$ both ψ and ϕ vanish identically. In the interval $[-y_{max}, y_{max}]$ we choose a set of uniformly spaced grid-points defined by y_j, $j=-N, -N+1, \cdots, -1, 0, 1, \cdots, N-1, N$, where $y_j=(j/N)y_{max}$. We can now write the equations in the two fluid regions and the boundary conditions at $y=0$ using finite-difference approximations. The difficulty is in imposing the boundary conditions at the interface for the fourth-order equation for ψ and obtaining a non-singular $\boldsymbol{B}$ matrix needed for solving the generalized eigenvalue problem. In the Appendix, we give the details of the finite-difference scheme we have used which overcomes these difficulties.

The spectrum of eigenvalues C_1 is determined by the set of parameters r, m, χ, S, M, P_2 and α. Furthermore, y_{max} and N must be chosen sufficiently large for convergence. For $r=1$, $m=1$, $\chi=2$, $S=0$, $M=0$, $P_2=0.025$ and $\alpha=10$, we have computed the spectrum with various values of y_{max} and N. In each case, we obtain only one growing mode, while the rest of the modes are damped. It is found that $y_{max}=6$ and $N=120$ are sufficient to give the growth rate of the unstable mode correct to 3 significant figures. As α becomes large, the numerical results should tend towards the short wavelength results. To check this, we vary α keeping all other parameters unchanged. The results of the numerical and short-wavelength calculations are shown in table 1.

It can be seen that for $\alpha = 10$, the numerical and short-wavelength results differ by about 3% while for $\alpha = 40$ the two agree to 3 significant figures. We further observe that, in this range of wavenumbers, the growth rate $\mathrm{Im}(C_1)$ increases with decrease in α. The question naturally arises as to whether this trend continues for smaller values of α. To check this, we carry out numerical runs for $\alpha = O(1)$ and $\alpha \ll 1$ with different values of χ and all other parameters unchanged. The results for $\chi = 1.5$, 2.0 and 3.0 are shown in figure 2(*a*). Although the analytical study assumed a short-wavelength approximation, the numerical results show that the instability is present even up to perturbations of long wavelength. Furthermore, the growth rate reaches a maximum for a value of α which is $O(1)$. Figure 2(*a*) also shows that the maximum growth rate occurs for shorter wavelengths as χ increases. This trend is further confirmed by figure 2(*b*) for $\chi = 1.01$ and figure 2(*c*) for $\chi = 100$. Next, we study the effect of varying P_2. In figure 3 we plot the growth rates against wavenumber for $P_2 = 1$ and $P_2 = 10$ for $\chi = 2$ with all other parameters the same as before. To study the effect of viscosity ratio, we have computed growth rates for $m = 0.1$ and $m = 10$ with $r = 1$, $\chi = 2$, $S = 0$, $M = 0$ and $P_2 = 0.025$. The results are shown in figure 4. Again, we find maximum growth rate for $\alpha = O(1)$ and agreement with (3.3) for short wavelengths. The largest growth rate shifts to longer wavelengths with increase in P_2 or decrease in m.

We have also computed the eigenfunction. With $r = 1$, $m = 1$, $\chi = 2$, $S = 0$, $M = 0$ and $P_2 = 0.025$, we have computed $\psi(y)$ and $\phi(y)$ for the unstable mode and we find that ψ is purely imaginary while ϕ is real, which means that ψ and ϕ are 90° out of phase. The profiles of $\mathrm{Im}[\psi(y)]$ and $\mathrm{Re}[\phi(y)]$ for the unstable mode for $\alpha = 10$, 1, 0.1 are shown in figure 5. We observe that both ψ and ϕ become small as we approach $\pm y_{max}$, justifying our truncating the solutions outside these limits. These plots also show the importance of rescaling the coordinates using the wavenumber. In the rescaled coordinates, the lengthscale of the unstable mode, in a direction normal to the interface, is of order unity even for wavenumbers differing by orders of magnitude.

Next, we study the effect of the surface tension parameter S. We first consider short-wavelength perturbations with $\alpha = 10$ and, for comparison with the analytical results, we choose S such that $\alpha^3 S = O(1)$. For $r = 1$, $m = 1$, $\chi = 2$, $M = 0$ and $P_2 = 0.025$, we compute the growth rate for different values of S. The results are given in table 2. Again, we observe good agreement between the numerical and short-wavelength results. The short-wavelength calculation predicts that $S = 0.0005$ is sufficient to stabilize the configuration. Numerical calculations indicate that stabilization occurs for $S = 0.00050045$. We now relax the requirement of short wavelength. The effect of surface tension on the growth rate of the instability is shown in figure 6. As expected, the stabilizing effect of surface tension becomes much smaller as the wavelength of the mode increases. We observe that while for $\alpha = 10$, stabilization occurs for $S \approx 0.0005$, for $\alpha = 1$, we require $S \approx 0.5$. Thus, although the short wavelength analysis predicts that surface tension has a very strong stabilizing effect, the numerical results show that stabilization is much weaker for $\alpha = O(1)$ at which the instability has maximum growth rate. Therefore, the instability due to a jump in magnetic diffusivity can persist for $\alpha = O(1)$ even when the surface tension parameter S is quite large.

Finally, we study the effect of the magnetic parameter M. Again, we consider short-wavelength perturbations with $\alpha = 10$ and for consistency with analytical calculations we choose M such that $\alpha M = O(1)$. For $r = 1$, $m = 1$, $\chi = 2$, $S = 0$, $P_2 = 0.025$ and $\alpha = 10$, we study the effect of variation in M on the growth rate. The results are

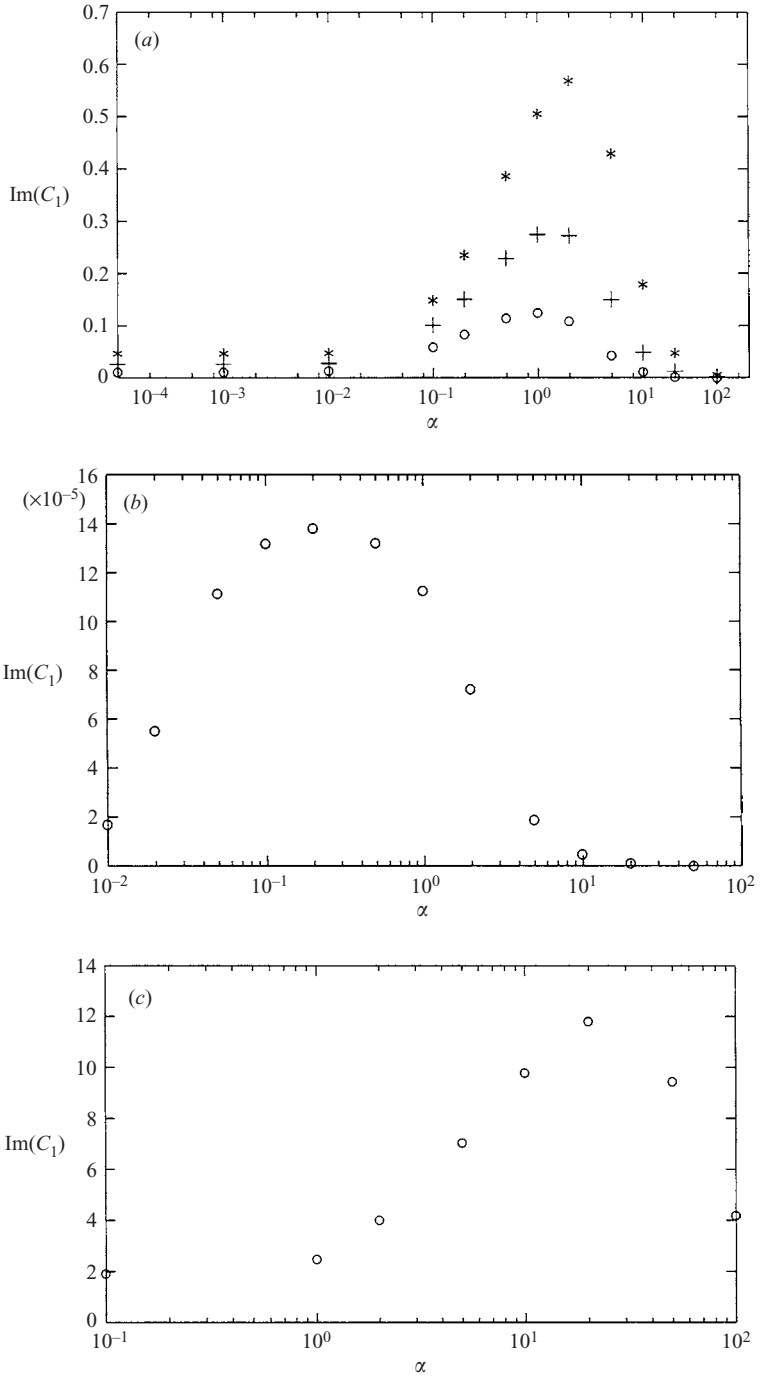

FIGURE 2. Growth rate Im(C_1) *vs.* wavenumber α for different magnetic diffusivity ratios (*a*) ○, $\chi = 1.5$; +, 2.0; ∗, 3.0, (*b*) $\chi = 1.01$, (*c*) $\chi = 100$ and with $r = 1$, $m = 1$, $S = 0$, $M = 0$ and $P_2 = 0.025$.

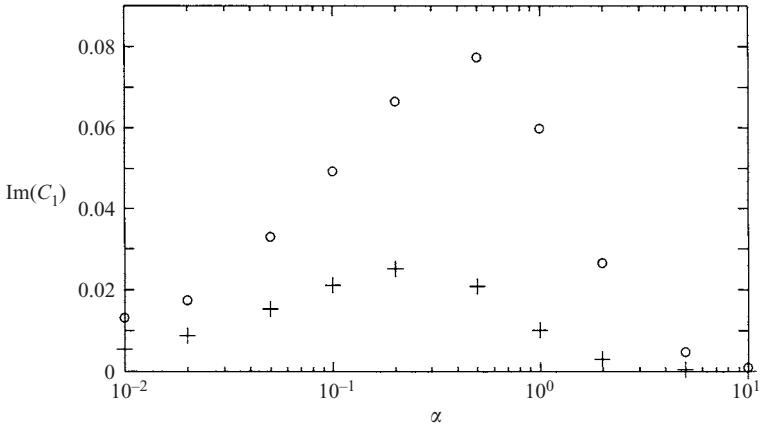

FIGURE 3. Growth rate Im(C_1) *vs.* wavenumber α for different magnetic Prandtl numbers, ○, $P_2 = 1$; +, 10, and with $r = 1$, $m = 1$, $\chi = 2$, $S = 0$ and $M = 0$.

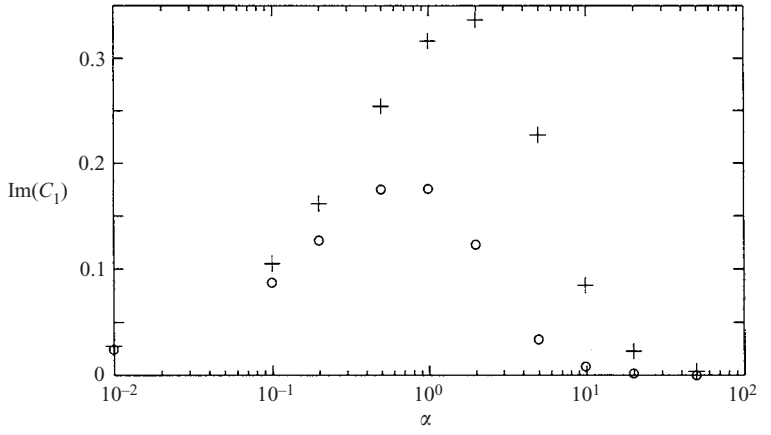

FIGURE 4. Growth rate Im(C_1) *vs.* wavenumber α for different viscosity ratios, ○, $m = 0.1$; +, 10, and with $r = 1$, $\chi = 2$, $S = 0$, $M = 0$ and $P_2 = 0.025$.

	Im(C_1)	
S	Numerical	Short wavelength
0.0	0.04850	0.05
0.0001	0.03892	0.04
0.0002	0.02928	0.03
0.0003	0.01959	0.02
0.0004	0.00984	0.01
0.0005	0.00004	0.0
0.0006	−0.00981	−0.01

TABLE 2. Effect of surface tension parameter S on the growth rate Im(C_1) for $r = 1$, $m = 1$, $\chi = 2$, $M = 0$ and $P_2 = 0.025$ and wavenumber $\alpha = 10$.

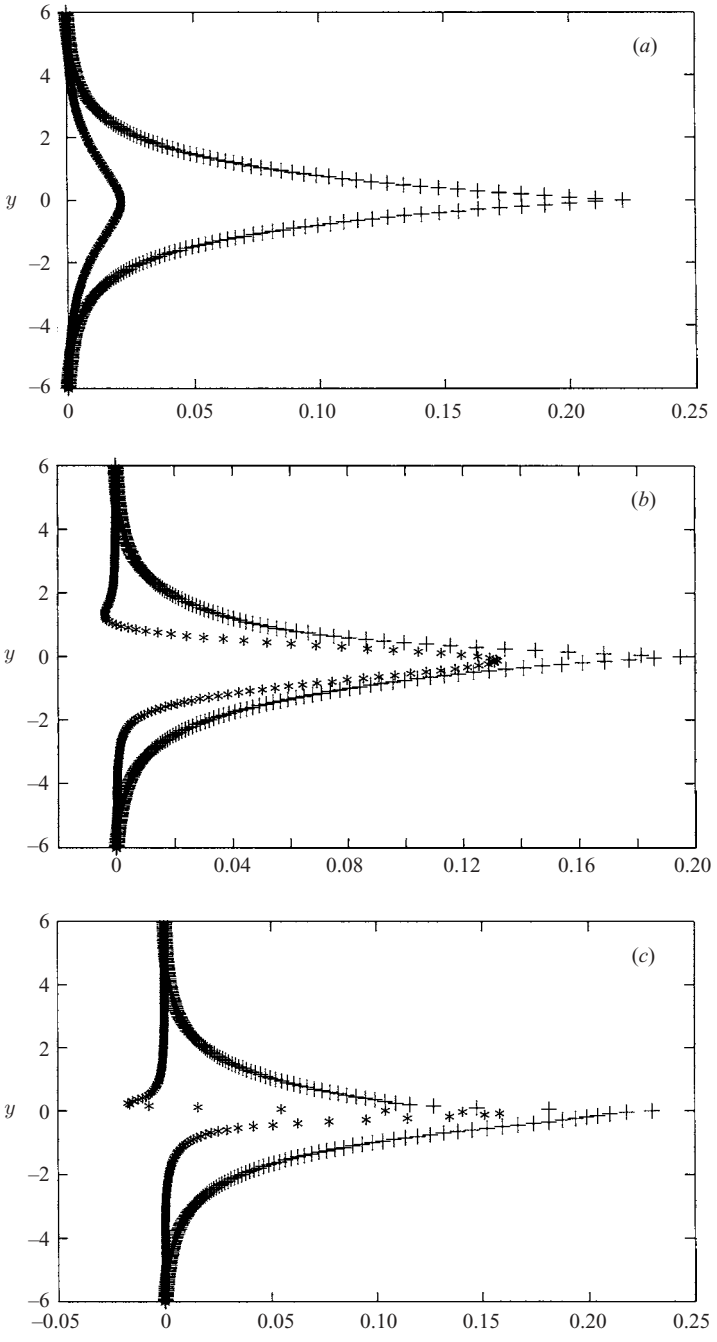

FIGURE 5. Eigenfunctions *, Im[$\psi(y)$] and +, Re[$\phi(y)$] for different wavenumbers (*a*) $\alpha = 10$, (*b*) $\alpha = 1$, (*c*) $\alpha = 0.1$ and with $r = 1$, $m = 1$, $\chi = 2$, $S = 0$, $M = 0$ and $P_2 = 0.025$.

shown in table 3. Again, there is good agreement between the numerical and short-wavelength results. While the short wavelength analysis predicts that stabilization occurs at $M = -0.05$, the numerical study predicts stabilization at $M = -0.050045$. We have also carried out numerical studies for disturbances of arbitrary

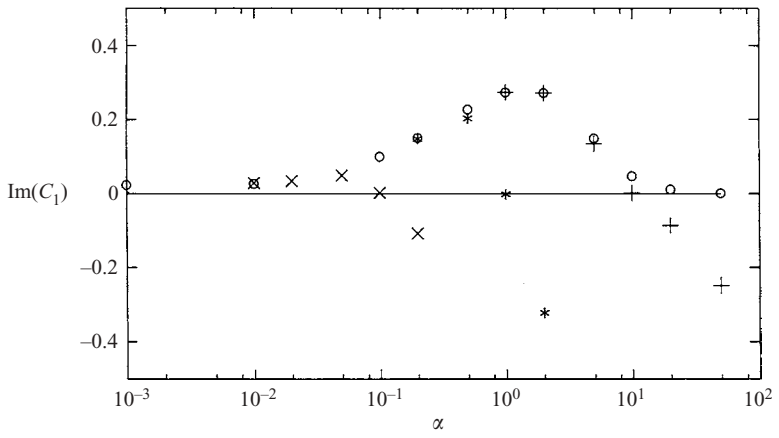

FIGURE 6. Growth rate Im(C_1) *vs.* wavenumber α for different values of the surface tension parameter S and with $r = 1$, $m = 1$, $\chi = 2$, $M = 0$ and $P_2 = 0.025$. ○, $S = 0$; +, 0.0005; ∗, 0.5; ×, 500.

	Im(C_1)	
M	Numerical	Short wavelength
0.10	0.14020	0.15
0.05	0.09524	0.10
0.0	0.04850	0.05
−0.04	0.00987	0.01
−0.05	0.00004	0.0
−0.06	−0.00985	−0.01
−0.10	−0.05005	−0.05

TABLE 3. Effect of magnetic parameter M on the growth rate Im(C_1) for $r = 1$, $m = 1$, $\chi = 2$, $S = 0$ and $P_2 = 0.025$ and wavenumber $\alpha = 10$.

wavelengths. The effect of the magnetic parameter on the growth rate of the instability is shown in figure 7. Again, for $\alpha = O(1)$ the effect of M is weaker than for short wavelengths. However, the variation with wavenumber is not as significant as for surface tension.

Thus, our numerical study confirms the results of the short-wavelength calculations. It also shows that the maximum growth rate occurs for $\alpha = O(1)$. In the short wavelength study, $\alpha \to \infty$, it was also assumed that $\alpha M = O(1)$ and $\alpha^3 S = O(1)$, from which it is not clear what values of α, M and S would be appropriate for these results to be valid. The numerical study shows that for some chosen values of α, M and S we do obtain an instability. It can also be seen that surface tension which had a very strong stabilizing effect for short-wavelength perturbations has a far weaker effect on the modes which have the largest growth rate, which suggests that it might be possible to observe this instability experimentally. In the next section, we discuss how the fluids should be chosen in order to study this instability in an experimental set-up. The numerical method in this section can be used to ensure that the parameters are suitably chosen so that we obtain an instability.

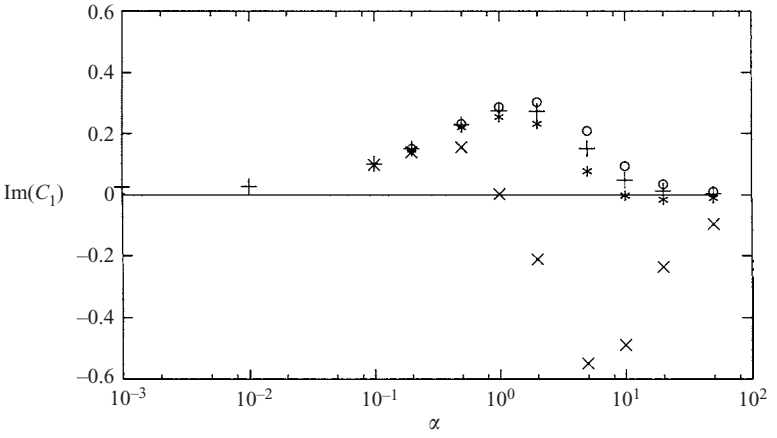

FIGURE 7. Growth rate $\mathrm{Im}(C_1)$ *vs.* wavenumber α for different values of the magnetic parameter M and with $r = 1$, $m = 1$, $\chi = 2$, $S = 0$ and $P_2 = 0.025$. ○, $M = 0.05$; +, 0; ∗, −0.05; ×, −0.5.

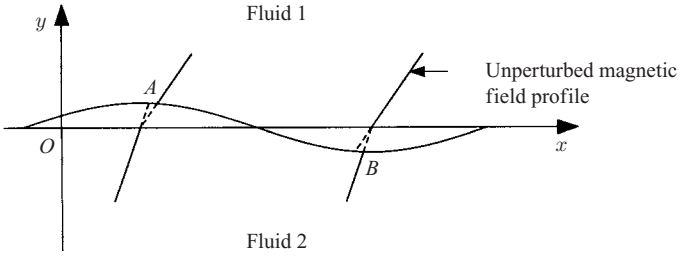

FIGURE 8. A sketch of the perturbed interface.

5. Physical explanation of the instability

In this section, we give an explanation of the mechanism of the instablity. Let us consider the case $M > 0$ and $\chi - 1 > 0$ (i.e. $s_1 > s_2$). We imagine that the interface is slightly perturbed as in figure 8. Since $s_1 > s_2$, at the point A where the interface is displaced upwards, the unperturbed magnetic field in fluid 1 is larger than that in fluid 2. Continuity of the tangential component of the magnetic field at the interface requires existence of perturbations in the magnetic field such that the perturbation should be in the negative x-direction in fluid 1 and in the positive x-direction in fluid 2. Such a magnetic field can be produced by a perturbation current $\boldsymbol{j}$ flowing in the positive z-direction, as shown in figure 9. Owing to the presence of the magnetic field B_0 in the positive x-direction, the Lorentz force will act in the positive y-direction leading to the displacement of the interface at A further upwards. Similarly, at the point B, where the interface is displaced downwards, the directions of the magnetic perturbations on both sides of the interface are reversed. The resulting current in the presence of the magnetic field $B_0\boldsymbol{e}_x$ then leads to a Lorentz force which tends to push the interface further downwards. Thus, we find that a small disturbance at the interface tends to grow and cause instability.

When $M > 0$ and $\chi - 1 < 0$ (i.e. $s_1 < s_2$), the directions of perturbations in the magnetic field along the x-direction on both sides of the disturbed interface will be reversed. Consequently, the direction of the Lorentz force is also reversed and it will push the peak A of the perturbed interface downwards and the trough B upwards.

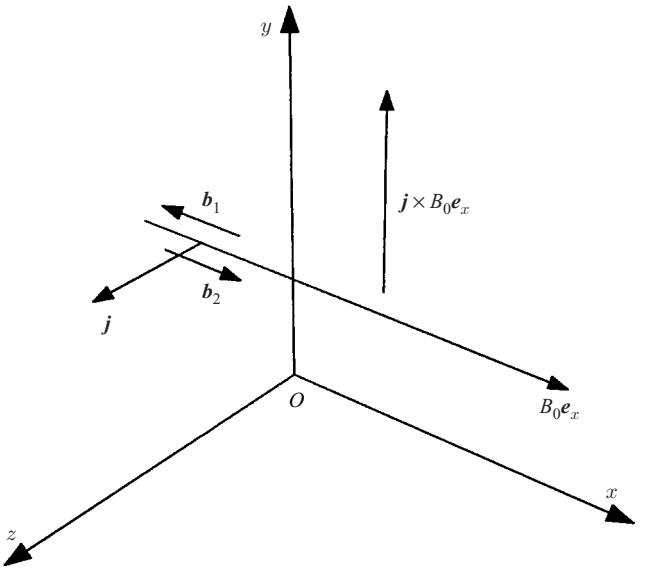

FIGURE 9. Generation of Lorentz force at the perturbed interface.

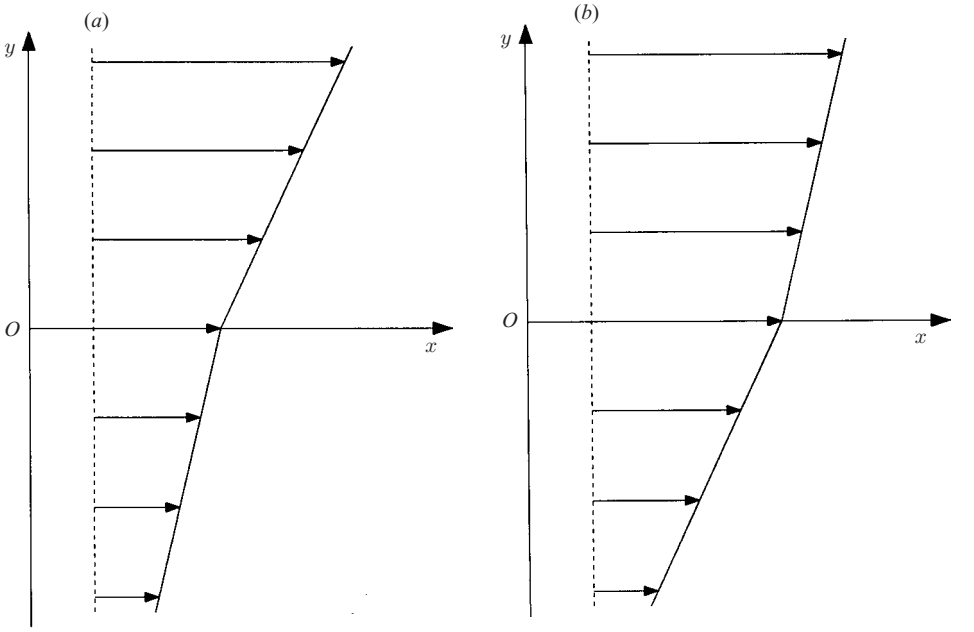

FIGURE 10. Different cases of the sheared magnetic field (*a*) $\chi > 1$, unstable, (*b*) $\chi < 1$, stable.

Evidently, in this case there will be stabilization. The two cases discussed are shown in figure 10. These are the only two cases possible for $\chi \neq 1$ if we assume that $M > 0$ and $s_1, s_2 > 0$. As explained in § 1, any other configuration can be made to satisfy these two conditions by an appropriate choice of coordinate system.

It will be noticed that our physical explanation does not require that the perturbation be of short wavelength. Therefore, a configuration which is unstable

would be expected to be unstable to perturbations of all wavelengths. This is confirmed by our numerical study.

There is one significant difference between our result and that of Hooper & Boyd (1983). In our analysis, the expression for the growth rate (3.3) contains a term involving the unperturbed magnetic field at the interface. This term has no counterpart in the result of Hooper & Boyd (1983). This is because the velocity at the interface can be removed by choosing a frame of reference which moves with the velocity of the fluid at the interface. However, the unperturbed magnetic field at the interface cannot be removed by a similar argument.

Finally, we suggest a set-up for experimental realization of the configuration studied in this paper. A constant electric field in the z-direction is produced by two conducting plates kept at two different potentials. This electric field will produce a constant current density in the z-direction, which will be different in the two fluids owing to the different values of electrical conductivity. If the experimental configuration is very long in the x-direction compared to the y-direction, this current will produce a magnetic field in the x-direction sheared in the y-direction. The magnetic shear will be proportional to the current density which will be proportional to the electrical conductivity and inversely proportional to the magnetic diffusivity. Therefore, boundary condition (2.13) will be automatically satisfied. It should be mentioned that the distance between the plates must be large for the two-dimensional model to be valid.

For the experimental study, it would be desirable to eliminate the destabilizing effect of viscosity difference and the stabilizing or destabilizing effect of the density difference of the two fluids. Since we do not have an unperturbed shear flow, difference in viscosities does not drive an instability, it merely influences the growth rate of the instability because of difference in electrical conductivity. In the presence of gravity, density difference would have a stabilizing or destabilizing effect. To eliminate this, it would be desirable to have two fluids which have the same density but different electrical conductivities. This might be possible if one of the fluids is a mixture whose composition can be chosen such that its density matches that of the other fluid.

6. Discussion

It is shown that an unbounded configuration of two viscous electrically conducting fluids permeated by a sheared magnetic field is always unstable for short-wavelength disturbances (in the absence of surface tension) if the magnetic field vanishes at the interface and the magnetic diffusivities of the two fluids are different. Instability may or may not occur if the field does not vanish at the interface and there is no instability if the magnetic diffusivities of the two fluids are equal. An experimental set-up for the realization of the sheared magnetic field assumed in the analysis is described.

One limitation of our analysis is that it is confined to two-dimensional disturbances. In this paper our aim was to demonstrate the existence of a new instability and for this a study of two-dimensional disturbances suffices. However, the question remains whether there can exist three-dimensional disturbances which have a faster growth rate and this needs further investigation.

We now compare our work with earlier studies of instabilities of the interface between two fluids with different electrical conductivities, in the context of aluminium reduction cells. Sneyd (1985) considered the situation where the equilibrium current is in a direction perpendicular to the interface between the two fluids, unlike the

present study where the equilibrium current is parallel to the interface. The instability occurs because a perturbation of the interface causes perturbation in layer thickness, leading to redistribution of electric current with consequent change in the Lorentz force. Therefore, the mechanism of instability requires a finite layer thickness. Sneyd (1992) generalized this study to include a horizontal component of current in one of the fluids and found instability driven by vertical gradients of the horizontal magnetic field. However, again this instability disappears when the layer depth is infinite and is, therefore, different from the instability discussed in this paper. Further, Sneyd & Wang (1994) showed that in an aluminium reduction cell carrying a uniform normal current, instability can occur on the cryolite/aluminium interface owing to mode interactions, the electromagnetic perturbation force due to one mode feeding energy into the other. More recently, Davidson & Lindsay (1998) have studied interfacial waves in aluminium reduction cells under the influence of vertical current density and found unstable travelling waves under certain conditions. Again, these become stable when the boundaries are removed. Therefore, in contrast to earlier studies, we obtain an instability which does not require the presence of physical boundaries. Moreover, in the short-wavelength approximation, we obtain a simple expression for growth rate which clearly shows that the instability is due to a jump in magnetic diffusivities. This does not seem to have been brought out in any of the earlier studies.

Again, a continuous variation in the electrical conductivity is known to give rise to a rippling instability. In a pioneering study, Furth *et al.* (1963) showed that a plasma which is stable in the ideal magnetohydrodynamic model may become unstable if the plasma is considered resistive. They identified three such resistive instabilities. One of these is the rippling instability which occurs when there is a gradient in the electrical conductivity. All these instabilities require the presence of a resonant layer given by $\boldsymbol{k}\cdot\boldsymbol{B}=0$, where $\boldsymbol{k}$ is the wavenumber of the mode and $\boldsymbol{B}$ is the magnetic field, and there is a thin resistive layer in the neighbourhood of the resonance. By contrast, in our study, the wavenumber has a component α along the magnetic field and we find instability even when α is large and the magnetic field does not vanish, though the growth rate is not as large as for the resistive instabilities found by Furth *et al.* (1963).

Appendix. The finite-difference scheme

In order to solve the equations for linear stability in an infinite region using the finite-difference method, as discussed in §4, we choose a large value of y_{max} and on the interval $[-y_{max}, y_{max}]$ we choose a set of uniformly spaced grid-points defined by y_j, $j=-N, -N+1, \cdots, -1, 0, 1, \cdots, N-1, N$, where $y_j=(j/N)y_{max}$. The values of ψ and f at grid-points y_j are denoted by $\psi_{1,j}$ and $f_{1,j}$ for $1\leqslant j\leqslant N$ and $\psi_{2,j}$ and $f_{2,j}$ for $-N\leqslant j\leqslant -1$. Using (2.34) and (2.39), we define ψ_0 and f_0 to be the values of ψ and f, identical for both fluids, at $y=0$. Using second-order-accurate central difference approximations, the finite-difference approximations for equations (2.30)–(2.33) can be readily written as

$$[\psi_{1,j-2}-(4+2h^2)\psi_{1,j-1}+(6+4h^2+h^4)\psi_{1,j}-(4+2h^2)\psi_{1,j+1}+\psi_{1,j+2}]$$
$$+\frac{\mathrm{i}h^2}{\alpha^2 P_2}m(\alpha M+\chi y_j)[f_{1,j-1}-(2+h^2)f_{1,j}+f_{1,j+1}]$$
$$=-C_1\frac{\mathrm{i}h^2}{\alpha^2 P_2}\frac{m}{r}[\psi_{1,j-1}-(2+h^2)\psi_{1,j}+\psi_{1,j+1}], \quad \text{(A 1)}$$

$$[\psi_{2,j-2}-(4+2h^2)\psi_{2,j-1}+(6+4h^2+h^4)\psi_{2,j}-(4+2h^2)\psi_{2,j+1}+\psi_{2,j+2}]$$
$$+\frac{\mathrm{i}h^2}{\alpha^2 P_2}(\alpha M+y_j)[f_{2,j-1}-(2+h^2)f_{2,j}+f_{2,j+1}]$$
$$=-C_1\frac{\mathrm{i}h^2}{\alpha^2 P_2}[\psi_{2,j-1}-(2+h^2)\psi_{2,j}+\psi_{2,j+1}], \quad (A\,2)$$

$$f_{1,j-1}-(2+h^2)f_{1,j}+f_{1,j+1}+\frac{\mathrm{i}h^2}{\alpha^2}\chi(\alpha M+\chi y_j)\psi_{1,j}=-C_1\frac{\mathrm{i}h^2}{\alpha^2}\chi f_{1,j}, \quad (A\,3)$$

$$f_{2,j-1}-(2+h^2)f_{2,j}+f_{2,j+1}+\frac{\mathrm{i}h^2}{\alpha^2}(\alpha M+y_j)\psi_{2,j}=-C_1\frac{\mathrm{i}h^2}{\alpha^2}f_{2,j}. \quad (A\,4)$$

Equation (A 3) is imposed at grid-points $j=1,\cdots,N$ and (A 4) at $j=-N,\cdots,-1$. It is assumed that $f_{1,N+1}=f_{2,-N-1}=0$ and $f_{1,0}=f_{2,0}=f_0$. Similarly, (A 1) and (A 2) are imposed at grid-points $j=2,\cdots,N$ and $j=-N,\cdots,-2$, where it is further assumed that $\psi_{1,N+1}=\psi_{1,N+2}=\psi_{2,-N-1}=\psi_{2,-N-2}=0$ and $\psi_{1,0}=\psi_{2,0}=\psi_0$. The difficulty in using (A 1) at $j=1$ is that this would require $\psi_{1,-1}$ which is not defined. A similar difficulty is encountered for (A 2) at $j=-1$. To overcome this problem we define

$$\Omega_0=\left(\frac{\mathrm{d}^2\psi_2}{\mathrm{d}y^2}\right)_{y=0}. \quad (A\,5)$$

Then, from (2.36) we obtain

$$\left(\frac{\mathrm{d}^2\psi_1}{\mathrm{d}y^2}\right)_{y=0}=m\Omega_0+(m-1)\psi_0. \quad (A\,6)$$

We can now write the finite-difference approximations for (2.30) at $j=1$

$$h^2 m\Omega_0+h^2(m-1)\psi_0-(2+2h^2)\psi_0+(5+4h^2+h^4)\psi_{1,1}$$
$$-(4+2h^2)\psi_{1,2}+\psi_{1,3}+\frac{\mathrm{i}h^2}{\alpha^2 P_2}m(\alpha M+\chi y_1)[f_0-(2+h^2)f_{1,1}+f_{1,2}]$$
$$=-C_1\frac{\mathrm{i}h^2}{\alpha^2 P_2}\frac{m}{r}[\psi_0-(2+h^2)\psi_{1,1}+\psi_{1,2}], \quad (A\,7)$$

and for (2.31) at $j=-1$

$$h^2\Omega_0-(2+2h^2)\psi_0+(5+4h^2+h^4)\psi_{2,-1}-(4+2h^2)\psi_{2,-2}$$
$$+\psi_{2,-3}+\frac{\mathrm{i}h^2}{\alpha^2 P_2}(\alpha M+y_{-1})[f_{2,-2}-(2+h^2)f_{2,-1}+f_0]$$
$$=-C_1\frac{\mathrm{i}h^2}{\alpha^2 P_2}[\psi_{2,-2}-(2+h^2)\psi_{2,-1}+\psi_0]. \quad (A\,8)$$

In order to write finite-difference approximations for the remaining boundary conditions (2.35), (2.37) and (2.38), we use second-order one-sided difference approximations for first derivatives and obtain

$$-\psi_{2,-2}+4\psi_{2,-1}-6\psi_0+4\psi_{1,1}-\psi_{1,2}=0, \quad (A\,9)$$

$$-6\Omega_0+\frac{1}{mh^2}[-3h^2(m-1)\psi_0+(4+9h^2)\psi_0-(9+12h^2)\psi_{1,1}+(6+3h^2)\psi_{1,2}-\psi_{1,3}]$$
$$-\frac{1}{h^2}[-(4+9h^2)\psi_0+(9+12h^2)\psi_{2,-1}-(6+3h^2)\psi_{2,-2}+\psi_{2,-3}]$$
$$+\frac{\mathrm{i}}{\alpha^2P_2}\left[\frac{C_1}{r}(-3\psi_0+4\psi_{1,1}-\psi_{1,2})+\left(\alpha M-\frac{S\alpha^3}{\chi-1}\right)(-3f_0+4f_{1,1}-f_{1,2})-2h\chi f_0\right]$$
$$-\frac{\mathrm{i}}{\alpha^2P_2}\left[C_1(3\psi_0-4\psi_{2,-1}+\psi_{2,-2})+\left(\alpha M-\frac{S\alpha^3}{\chi-1}\right)(3f_0-4f_{2,-1}+f_{2,-2})-2hf_0\right]=0, \quad \text{(A 10)}$$

$$2h(\chi-1)\psi_0=C_1(f_{2,-2}-4f_{2,-1}+6f_0-4f_{1,1}+f_{1,2}). \quad \text{(A 11)}$$

We now need to collect the finite-difference equations to form the generalized matrix eigenvalue problem. The first difficulty is that (A 9) does not involve C_1 and, therefore, would lead to a row of zeros in matrix $\boldsymbol{B}$, making it singular. To overcome this, we solve (A 9) for ψ_0 and substitute this into the remaining equations. Further, we observe that there are no terms corresponding to Ω_0 in the matrix $\boldsymbol{B}$. This implies a column of zeros in matrix $\boldsymbol{B}$ making it singular. To overcome this, we solve (A 10) for Ω_0 and substitute it into the remaining equations. We are now left with a set of $4N+1$ equations, namely (A 1) for $j=2,\cdots,N$, (A 2) for $j=-N,\cdots,-2$, (A 3) for $j=1,\cdots,N$, (A 4) for $j=-N,\cdots,-1$ and equations (A 7), (A 8) and (A 11), involving $4N+1$ variables, namely, $\psi_{1,j}$ $(j=1,\cdots,N)$, $\psi_{2,j}$ $(j=-N,\cdots,-1)$, $f_{1,j}$ $(j=1,\cdots,N)$, $f_{2,j}$ $(j=-N,\cdots,-1)$ and f_0, in the form of a generalized matrix eigenvalue problem of the form $\boldsymbol{Ax}=C_1\boldsymbol{Bx}$ where the matrix $\boldsymbol{B}$ is now non-singular. This can be solved using readily available library routines.

REFERENCES

Chandrasekhar, S. 1981 *Hydrodynamic and Hydromagnetic Stability*. Dover.

Davidson, P. A. & Lindsay, R. I. 1998 Stability of interfacial waves in aluminium reduction cells. *J. Fluid Mech.* **362**, 273–295.

Drazin, P. G. & Reid, W. H. 1981 *Hydrodynamic Stability*. Cambridge University Press.

Fejer, J. A. 1964 Hydromagnetic stability of a fluid velocity discontinuity between compressible fluids. *Phys. Fluids* **7**, 499–503.

Furth, H. P., Killeen, J. & Rosenbluth, M. N. 1963 Finite-resistivity instabilities of a sheet pinch. *Phys. Fluids* **6**, 459–484.

Hickox, C. E. 1971 Instability due to viscosity and density stratification in axisymmetric pipe flow. *Phys. Fluids* **14**, 251–262.

Hinch, E. J. 1984 A note on the mechanism of the instability at the interface between two shearing fluids *J. Fluid Mech.* **144**, 463–465.

Hooper, A. P. & Boyd, W. G. C. 1983 Shear-flow instability at the interface between two viscous fluids *J. Fluid Mech.* **128**, 507–528.

Li, C.-H. 1969 Instability of three-layer viscous stratified flow. *Phys. Fluids* **12**, 2473–2481.

Li, J., Renardy, Y. Y. & Renardy, M. 1998 A numerical study of periodic disturbances on two-layer Couette flow. *Phys. Fluids* **10**, 3056–3071.

Lin, C. C. 1955 *Hydrodynamic Stability*. Cambridge University Press.

Renardy, Y. Y. & Li, J. 1999 Comment on 'A numerical study of periodic disturbances on two-layer Couette flow'. *Phys. Fluids* **11**, 3189–3190.

Shercliff, J. A. 1965 *A Textbook of Magnetohydrodynamics*. Pergamon.

Sneyd, A. D. 1985 Stability of fluid layers carrying a normal electric current. *J. Fluid Mech.* **156**, 223–236.

Sneyd, A. D. 1992 Interfacial instabilities in aluminium reduction cells. *J. Fluid Mech.* **236**, 111–126.

Sneyd, A. D. & Wang, A. 1994 Interfacial instability due to MHD mode coupling in aluminium reduction cells. *J. Fluid Mech.* **263**, 343–359.

White, R. B. 1989 *Theory of Tokamak Plasmas.* North-Holland.

Yih, C.-S. 1967 Instability due to viscosity stratification. *J. Fluid Mech.* **27**, 337–352.